

## X-ray Crystal Structure of Alcohol Products Bound at the Active Site of Soluble Methane Monooxygenase Hydroxylase

Douglas A. Whittington, Matthew H. Sazinsky, and Stephen J. Lippard\*

Department of Chemistry, Massachusetts Institute of Technology, Cambridge, Massachusetts 02139

Received August 25, 2000

Methane monooxygenases oxidize methane to methanol in bacteria that consume CH<sub>4</sub> as their sole source of carbon and energy.<sup>1</sup> The soluble methane monooxygenase (MMO) from the methanotrophic bacterium *Methylococcus capsulatus* (Bath) comprises three protein components. Carboxylate-bridged dinuclear iron centers, housed at active sites in the dimeric 251-kDa hydroxylase (MMOH) enzyme, activate dioxygen for subsequent oxidation of methane.<sup>2,3</sup> The structure of MMOH is known in two crystal forms from two organisms<sup>4–6</sup> in both its oxidized and reduced states.<sup>7</sup> Several solvent-occupied coordination positions at the active site are available for substrate or product binding, but to date no geometric information exists for such bound molecules. We report here X-ray crystal structures of MMOH from *M. capsulatus* (Bath) with methanol or ethanol bound at the dinuclear iron center.

MMOH has been extensively studied by various spectroscopic techniques, many of which have been used to probe the binding of small molecule substrates, inhibitors, and products at the active site. The binding of phenol, the product of benzene hydroxylation by the enzyme, to the oxidized diiron(III) center was identified on the basis of spectroscopic data.<sup>8</sup> Evidence for *trans*-1,2-dichloroethylene and tetrachloroethylene binding to the diiron(II) center in reduced MMOH in the presence of the coupling protein B was obtained by variable temperature/variable field circular dichroism and magnetic circular dichroism spectroscopy.<sup>9</sup> Electron nuclear double resonance (ENDOR) spectroscopic evidence also demonstrated that DMSO, acetate, and methanol bind to the mixed-valent Fe(II)Fe(III) form of MMOH.<sup>10,11</sup> ENDOR spectroscopy revealed that the mixed-valent diiron center can simultaneously accommodate DMSO, methanol, and a water molecule in addition to amino acid side-chain ligands that are always present. The only spectroscopic evidence for methanol and ethanol binding to the oxidized diiron(III) center comes from EPR spectra of protein that was reduced by  $\gamma$ -irradiation at 77 K to produce mixed-valent Fe(II)Fe(III) centers that maintained the geometry of the diiron(III) state.<sup>12,13</sup> Dramatic perturbations in the EPR spectra upon addition of methanol and ethanol strongly indicate ligation of the alcohols to the diiron(III) active site, a conclusion supported for ethanol by ENDOR spectroscopy.<sup>13</sup>

In the present work, we crystallized MMOH from *M. capsulatus* (Bath) in the orthorhombic crystal form having unit cell dimensions  $a = 72 \text{ \AA}$ ,  $b = 172 \text{ \AA}$ , and  $c = 222 \text{ \AA}$  by a modification<sup>14</sup> of the procedure previously reported.<sup>5</sup> The crystals were then soaked in stabilizing cryosolutions containing the mother liquor with 10% PEG 8000, 20% glycerol, and either 1.0 M methanol or 0.9 M ethanol. X-ray diffraction data were collected at 100 K on beamline 9-1 at the Stanford Synchrotron Radiation Laboratory. The X-ray data were scaled and merged using the HKL suite of programs,<sup>15</sup> and structures were refined using CNS.<sup>16,17</sup> Interactive model building was done with O.<sup>18</sup>

The structures of the methanol- and ethanol-containing MMOH resemble closely that of native, oxidized MMOH. Significant differences occur only at the active site in one of the two protomers of the dimeric enzyme and for the conformations of selected surface residues, which were less well defined in the alcohol-treated protein structures. Changes at the active site in the methanol-soaked crystals appeared as distinct difference Fourier electron density at a position bridging the two iron atoms in one protomer (Figure 1b), the same site occupied by bridging water in the low temperature *M. capsulatus* (Bath) structure.<sup>7</sup> The difference electron density between the iron atoms in the ethanol-treated crystals was correspondingly larger (Figure 1c).

We considered the possibility that the electron density attributed to methanol and ethanol might be an alternative arrangement of solvent at the active site. Modeling water in place of methanol resulted in unreasonably long Fe–O bonds of 2.6 and 2.7 Å and left residual electron density in difference Fourier maps. Modeling of a single water molecule in the bridging position of the ethanol structure also failed to account for all of the observed electron density, and introduction of two water molecules led to a refined separation of 2.3 Å, clearly too close to be realistic. Moreover, when methanol or ethanol were introduced, they both refined to reasonable positions with respect to the iron atoms, the electron density was adequately accounted for, and the *B* factors were good. *B*-values of ~45 and ~47 Å<sup>2</sup> for the methanol and ethanol, respectively, were in accord with the *B*-values of 40–48 Å<sup>2</sup> for the carboxylate moieties of Glu209 and Glu243. Ordered water molecules in the active site of the native, oxidized structure had *B*-values of 36–45 Å<sup>2</sup>.<sup>14</sup> Figure 2 gives the geometries of alcohol binding at the active site.<sup>19</sup>

The observation of bound product in only one of the two protomers in the MMOH dimer is consistent with prior results from EPR experiments on the cryoreduced enzyme.<sup>12</sup> Methanol binds to all diiron(III) centers, but in two major forms that are distinguished by EPR in the frozen, one-electron reduced MMOH. The absence of methanol in one of the protomers as revealed by the present X-ray diffraction work may reflect restricted access in the crystalline state or that methanol in one of the protomers is better ordered. Multiple populations of the diiron centers in

(1) Dalton, H. *Adv. Appl. Microbiol.* **1980**, *26*, 71–87.

(2) Liu, K. E.; Lippard, S. J. *Adv. Inorg. Chem.* **1995**, *42*, 263–289.

(3) Wallar, B. J.; Lipscomb, J. D. *Chem. Rev.* **1996**, *96*, 2625–2657.

(4) Rosenzweig, A. C.; Frederick, C. A.; Lippard, S. J.; Nordlund, P. *Nature* **1993**, *366*, 537–543.

(5) Rosenzweig, A. C.; Brandstetter, H.; Whittington, D. A.; Nordlund, P.; Lippard, S. J.; Frederick, C. A. *Proteins* **1997**, *29*, 141–152.

(6) Elango, N.; Radhakrishnan, R.; Froland, W. A.; Wallar, B. J.; Earhart, C. A.; Lipscomb, J. D.; Ohlendorf, D. H. *Protein Sci.* **1997**, *6*, 556–568.

(7) Rosenzweig, A. C.; Nordlund, P.; Takahara, P. M.; Frederick, C. A.; Lippard, S. J. *Chem. Biol.* **1995**, *2*, 409–418.

(8) Andersson, K. K.; Elgren, T. E.; Que, L., Jr.; Lipscomb, J. D. *J. Am. Chem. Soc.* **1992**, *114*, 8711–8713.

(9) Pulver, S. C.; Froland, W. A.; Lipscomb, J. D.; Solomon, E. I. *J. Am. Chem. Soc.* **1997**, *119*, 387–395.

(10) DeRose, V. J.; Liu, K. E.; Lippard, S. J.; Hoffman, B. M. *J. Am. Chem. Soc.* **1996**, *118*, 121–134.

(11) Hendrich, M. P.; Fox, B. G.; Andersson, K. K.; Debrunner, P. G.; Lipscomb, J. D. *J. Biol. Chem.* **1992**, *267*, 261–269.

(12) Davydov, R.; Valentine, A. M.; Komar-Panicucci, S.; Hoffman, B. M.; Lippard, S. J. *Biochemistry* **1999**, *38*, 4188–4197.

(13) Smoukov, S.; Kopp, D. A.; Valentine, A. M.; Lippard, S. J.; Hoffman, B. M. Submitted for publication.

(14) Whittington, D. A.; Lippard, S. J. *J. Am. Chem. Soc.* **2001**, In press.

(15) Otwinowski, Z.; Minor, W. *Methods Enzymol.* **1997**, *276*, 307–326.

(16) Brünger, A. T.; Adams, P. D.; Clore, G. M.; DeLano, W. L.; Gros, P.; Grosse-Kunstleve, R. W.; Jiang, J.-S.; Kuszewski, J.; Nilges, M.; Pannu, N. S.; Read, R. J.; Rice, L. M.; Simonson, T.; Warren, G. L. *Acta Crystallogr.* **1998**, *D54*, 905–921.

(17) Complete data collection and refinement statistics appear in Table S1, and details of the structure solution and refinement are provided in Supporting Information.

(18) Jones, T. A.; Zou, J.-Y.; Cowan, S. W.; Kjeldgaard, M. *Acta Crystallogr.* **1991**, *A47*, 110–119.

(19) NOTE ADDED IN PROOF: The 1.85 Å resolution X-ray structure of MMOH containing 2-bromoethanol bound in the same bridging position has just been determined (M.H. Sazinsky and S.J. Typard, unpublished results). The high electron density of the bromine atom in this structure leaves no doubt about the location of the alcohol molecule.

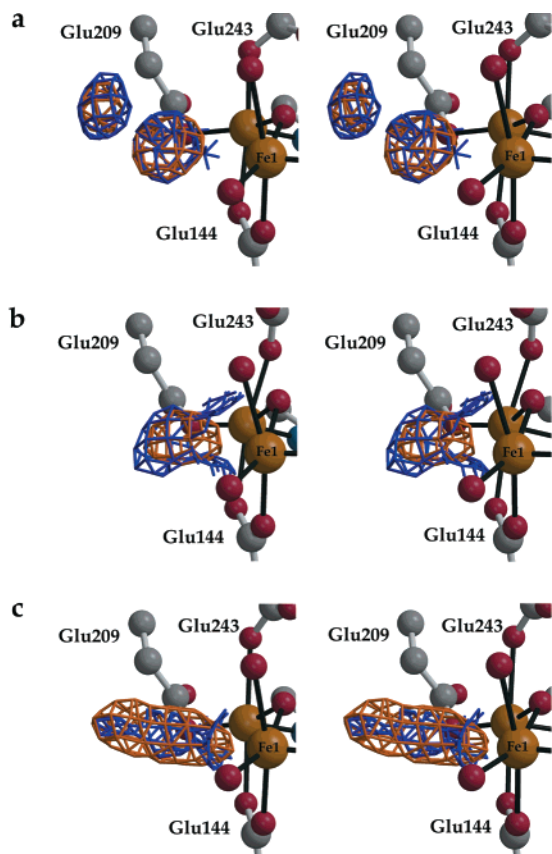


**Figure 1.** Stereoview of the active site of MMOH in the (a) native, oxidized (see ref 14), (b) methanol-soaked or (c) ethanol-soaked structures. Electron density for the bridging species is depicted from both a  $|2F_o| - |F_c|$  map (blue,  $1.2\sigma$  contour) and an  $|F_o| - |F_c|$  map (orange,  $4\sigma$  contour in a and b,  $3\sigma$  contour in c). The electron density in a–c is assigned respectively as hydroxide (with a tightly associated water molecule), methoxide, and ethanol. The maps were calculated from the final, refined models with the species occupying the coordination position distal to the His residues removed. The view is down the Fe–Fe vector.

MMOH have also been observed in Mössbauer and X-ray absorption spectroscopic experiments,<sup>20,21</sup> and X-ray crystallographic differences between the active sites in the two protomers of MMOH were reported previously.<sup>7</sup>

Comparison of the methanol- and ethanol-binding modes reveals one notable difference. Whereas ethanol binds strongly to Fe1 and weakly to Fe2, methanol occupies a bridging position symmetrically disposed between the two iron atoms. The 2.1 Å distances from each iron to the bridging oxygen atom and the symmetric nature of the bridge suggest that the ligand is methoxide and not methanol. Such an assignment affords charge neutrality to the diiron(III) site and is consistent with results of diiron coordination complexes listed in the Cambridge Structural Database, which reveals no dinuclear iron compound having a bridging methanol; only bridging methoxide is observed.<sup>22</sup> The  $pK_a$  value of methanol is 15.5, similar to that of water. A hydroxide bridge occurs in the same position in oxidized MMOH from *Methylosinus trichosporium* OB3b, and is consistent with density functional theoretical (DFT) considerations.<sup>6,23</sup> Protons on bridging water molecules have lower  $pK_a$  values than those at terminal positions, and similar behavior is expected for methanol.

(20) Liu, K. E.; Valentine, A. M.; Wang, D.; Huynh, B. H.; Edmondson, D. E.; Salifoglou, A.; Lippard, S. J. *J. Am. Chem. Soc.* **1995**, *117*, 10174–10185.

(21) Shu, L.; Liu, Y.; Lipscomb, J. D.; Que, L., Jr. *J. Biol. Inorg. Chem.* **1996**, *1*, 297–304.

(22) Allen, F. H.; Kennard, O. *Chem. Des. Autom. News* **1993**, *8*, 31–37.

(23) Dunitz, B. D.; Beachy, M. D.; Cao, Y.; Whittington, D. A.; Lippard, S. J.; Friesner, R. A. *J. Am. Chem. Soc.* **2000**, *122*, 2828–2839.

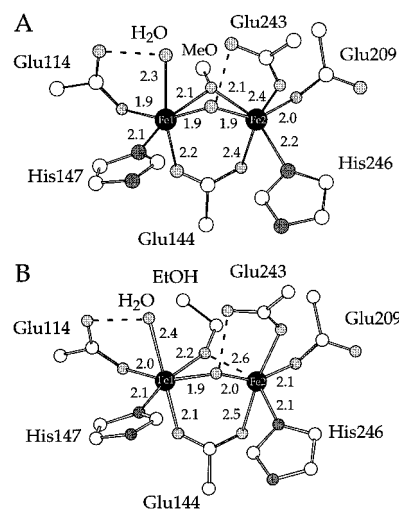


**Figure 2.** (A) Refined MMOH active site structure from the methanol-soaked crystals. Distances are labeled in Å. Dashed lines represent hydrogen bonds between Glu114 and the terminal water molecule (2.6 Å) and between Glu243 and the  $\mu$ -OH (2.6 Å). The Fe $\cdots$ Fe distance is 3.0 Å. (B) Refined MMOH active-site structure from the ethanol-soaked crystals. Distances are labeled in Å. The dashed lines represent hydrogen bonds from Glu114 to the terminal water molecule (2.5 Å) and Glu243 to the  $\mu$ -OH (2.8 Å), as well as the weak interaction between the oxygen atom of ethanol and Fe2 (2.6 Å). The Fe $\cdots$ Fe distance is 3.1 Å.

In contrast, the ethanol-binding mode is asymmetric and resembles that of a terminal water molecule found in previous high-resolution structures of reduced MMOH.<sup>7</sup> The observed bond distance of 2.2 Å to Fe1 is in agreement with values for iron coordination complexes that have terminal ethanol ligands, although an ethoxide ligand would provide charge neutrality and cannot be ruled out.

The observed binding sites for the alcohols in these structure determinations suggest that this position may be the point of product release in the catalytic mechanism. They further reinforce a finding of the DFT calculations that there is a strong preference for water to remain bound as a terminal ligand to Fe1 throughout the catalytic cycle.<sup>23</sup> In both of the present structures this water is clearly defined and hydrogen-bonded to Glu114 (Figure 2). Finally, the discovery of a bridging methanol is consistent with hydroxylation of methane by the di( $\mu$ -oxo)diiron(IV) intermediate Q in the catalytic cycle at a bridging oxo group, with this atom becoming the methanol oxygen atom. This conclusion was reached by recent DFT model studies of the methane hydroxylation reaction.<sup>24</sup>

**Acknowledgment.** This work was supported by a grant from the National Institutes of Health (GM32134 to S.J.L.). D.A.W. was partially supported by a NIH Biotechnology Training Grant. X-ray data were collected at the Stanford Synchrotron Radiation Laboratory (SSRL), which is funded by the Department of Energy (BES, BER) and the National Institutes of Health (NCR, NIGMS). Coordinates have been deposited in the RCSB databank, accession numbers 1FZ6 and 1FZ7 for the methanol- and ethanol-containing structures, respectively.

**Supporting Information Available:** A table containing data collection and refinement statistics for both structures, and details of the structure determinations (PDF). This material is available free of charge via the Internet at <http://pubs.acs.org>.

JA0031725

(24) Gherman, B. F.; Dunitz, B. D.; Whittington, D. A.; Lippard, S. J.; Friesner, R. A. Submitted for publication, and refs cited therein.